Pis'ma v ZhETF, vol. 89, iss. 4, pp. 198 – 203 © 2009 February 25

Evidence of maximum in the melting curve of hydrogen at megabar pressures

M. I. Eremets[1)]*, *I. A. Trojan**+

*Max Planck Institute für Chemie, 55020 Mainz, Germany

+A. V. Shubnikov Institute of Crystallography RAS, 117333 Moscow, Russia

Submitted 18 December 2008

Resubmitted 26 Janury 2009

Hydrogen at high pressures of $\sim$400 GPa might be in a zero-temperature *liquid* ground state (N. Ashcroft, J. Phys. Condens. Matter A **12**, 129 (2000), E. G. Brovman et al., Sov. Phys. JETP **35**, 783 (1972)). If metallic hydrogen is liquid, the melting $T_{\rm melt}(P)$ line should possess a maximum. Here we report on the experimental evaluation of the melting curve of hydrogen in the megabar pressure range. The melting curve of hydrogen has been shown to reach a maximum with $T_{\rm melt} = 1050 \pm 60$ K at $P = 106$ GPa and the melting temperature of hydrogen decreases at higher pressures so that $T_{\rm melt} = 880 \pm 50$ K at $P = 146$ GPa. The data were acquired with the aid of a laser heating technique where diamond anvils were not deteriorated by the hot hydrogen. Our experimental observations are in agreement with the theoretical prediction of unusual behavior of the melted hydrogen [S. Bonev et al., Nature **431**, 669 (2004)].

PACS: 62.50.–p, 64.70.dj, 67.63.Cd, 67.80.ff

1. Introduction. Establishing the melting curve of hydrogen is of fundamental interest in physics and astrophysics, as hydrogen is the simplest element and the most abundant matter in the interiors of stars and giant planets. Recent theoretical calculations show unusual behavior of the hydrogen melting curve: it starts at ambient pressure at 14 K, attains a maximum at $T \approx 900$ K at $P \approx 90$ GPa [1], and is extrapolated [2] to 0 K at $P \approx 400$ GPa, where hydrogen is predicted to be in liquid ground state [3, 4] as a metallic superfluid or superconducting superfluid [3, 5] (Fig.1). Thus, it is possible that fluid hydrogen occupies the bulk of the pressure–temperature (P, T) phase diagram, whereas the domain of solid hydrogen is limited by the melting curve (Fig.1). Above the melting curve, at megabar pressures hydrogen becomes gradually conductive and then metallic because of the dissociation of molecules and narrowing of the band gap due to delocalization of electrons (Fig.1: from Refs [1] (open diamond), [6] (solid square), [9] (circles), [7] (open square), and [12] (star). See also Refs. [8, 10, 11]. Therefore, hydrogen might already occur in its metallic state at accessible pressures of $P > 100$ GPa and temperatures of below $T = 2000$ K (Fig.1).

First-principles molecular dynamics simulations yield similar results [1, 6]; however, there exist contradictory explanations of the maximum in the melting curve. According to Ref. [6], a sharp liquid–liquid transition takes place between a molecular and a dissociated phase at $\approx$125 GPa and 1500–2000 K (Fig.1, solid square). The transition is accompanied by a volume reduction of $\approx$6%, thus explaining the negative slope of the melting curve at higher pressures. Based on two-phase simulations [1], a second physical origin of the maximum in the melt curve of hydrogen has been proposed: the contrasting rates at which the steep increase in repulsive interactions at high density are softened by attractive many-body interactions in the

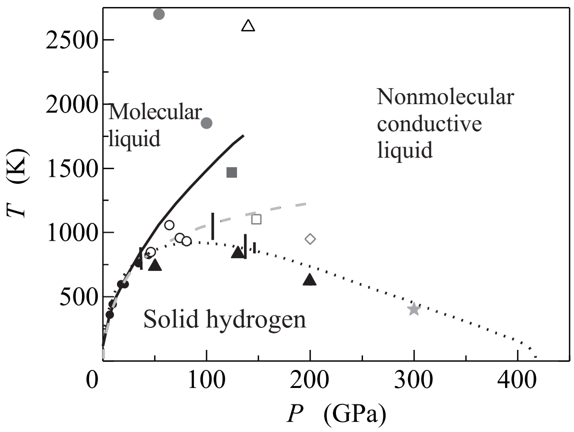

Fig.1. Phase diagram of hydrogen. Our melting points are shown with black bars. Domain of conductive fluid hydrogen is indicated by the shaded area. The provisional low-temperature boundary of this area is based on calculations (see text for details)

[1)]e-mail: eremets@mpch-mainz.mpg.de

solid and liquid phases as a function of pressure. Recent *ab initio* molecular-dynamics calculations also indicate a strong decline in the melting curve with pressure, showing stability of the liquid phase at 300 GPa and 400 K [12].

The melting curve of hydrogen has been studied experimentally by many authors, starting with the first measurements performed at the Leiden laboratory in the Netherlands, nearly 100 years ago for pressures up to 0.25 kbar [13]. The most recent measurements have been performed at up to 7.7 GPa and 373 K [14], 15.2 GPa and 530 K [15], 40 GPa and 800 K [16], and 80 GPa and 1100 K [17]. Solids and open circles on Fig.1 indicate experimental melting data from Refs [16] and [17]. Experimental data on melting are typically fitted to empirical melting laws that can be used for the analytical presentation and extrapolation. Those the most widely employed are the Simon–Glatzel [18] (Fig.1, the solid line) and Kraut–Kennedy [19] (Fig.1, the dashed line) expressions, which generally describe experimental melting curves with great accuracy. Both predict a continuous rise in the melting line. In contrast, the empirical Kechin melting equation [2] (Fig.1, the dot line) yields an excellent fit to experimental data but predicts a turnover in the melting curve at ~ 100 GPa and 950 K [2], close to the parameters of the maximum in the melting curve obtained via first-principles calculations [1] (Fig.1, the solid triangles). Available hydrogen melting data [15–17] clearly demonstrate a deviation from the common Simon–Glatzel law, while they can be satisfactory fitted to the Kraut–Kennedy equation (melting temperature is proportional to the isothermal volume compression) (Fig.1). The highest pressure of 80 GPa of the hydrogen melting curve have recently been achieved [17] using 70–200 ns laser pulses for heating. However, the temperature measurements and detection of the melt were not temporally resolved and determined indirectly from the data integrated over the laser pulses. The maximum in the melting curve was assigned to a sharp increase of the melting temperature at one point at 65 GPa. Other experimental points in this study satisfactorily agree with the Kraut-Kennedy equation [19]. To summarize, the pressure range of available experimental data [15–17] is insufficient for a reliable estimate of a maximum at the melting curve hydrogen and for extrapolation to higher pressures. Therefore only experiments conducted at significantly higher, megabar pressures can give an answer if melting temperature decreases with pressure, i.e. the melting curve has a maximum. So far experimental work on dense hydrogen in the megabar range has been limited to shock-wave experiments conducted at elevated temperatures [20, 21] (Fig.1, open triangle point). The melting curve was not determined in these studies, however, it was demonstrated that fluid hydrogen is conductive at $P \approx 150$ GPa and high temperatures of ≈ 3000 K.

The primary goal of the present static pressure work was to determine values of the melting temperature of hydrogen at pressure range up to about 150 GPa within which the predicted maximum at the melting curve [1] would be observable.

2. Experimental. We performed numerous laser heating runs in four different diamond anvil cells (DACs) loaded cryogenically with hydrogen. Experiments with hydrogen under high-temperature high-pressure conditions pose a number of significant difficulties. The most severe problem is the interaction of hydrogen with diamond anvils: the hot hydrogen easily penetrates diamond anvils causing their breakage to pieces. This inevitably happens at experiments with external heating

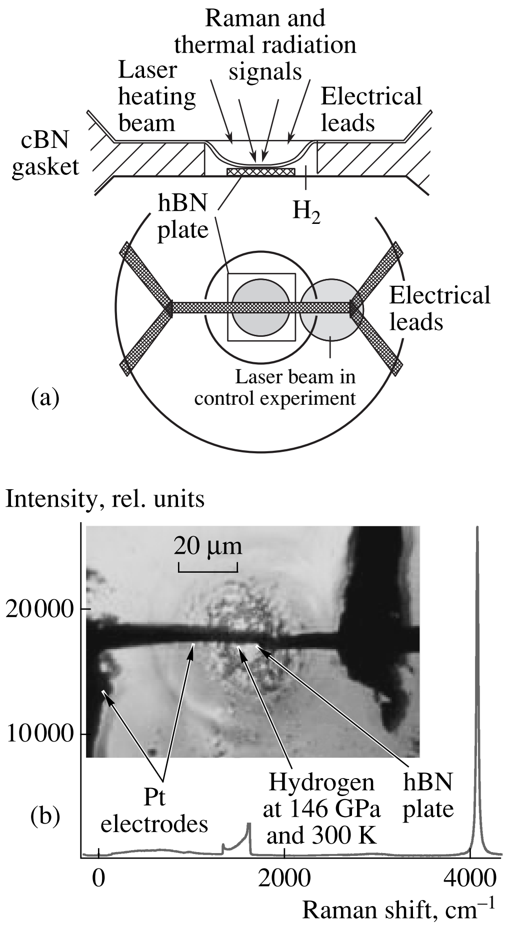

Fig.2. Arrangement of a diamond anvil cell for the experiment on the hydrogen melting. (a) Schematic diagram: side and top views. (b) The photograph of the diamond anvil cell and a Raman spectrum of hydrogen at 300 K and 146 GPa shown below

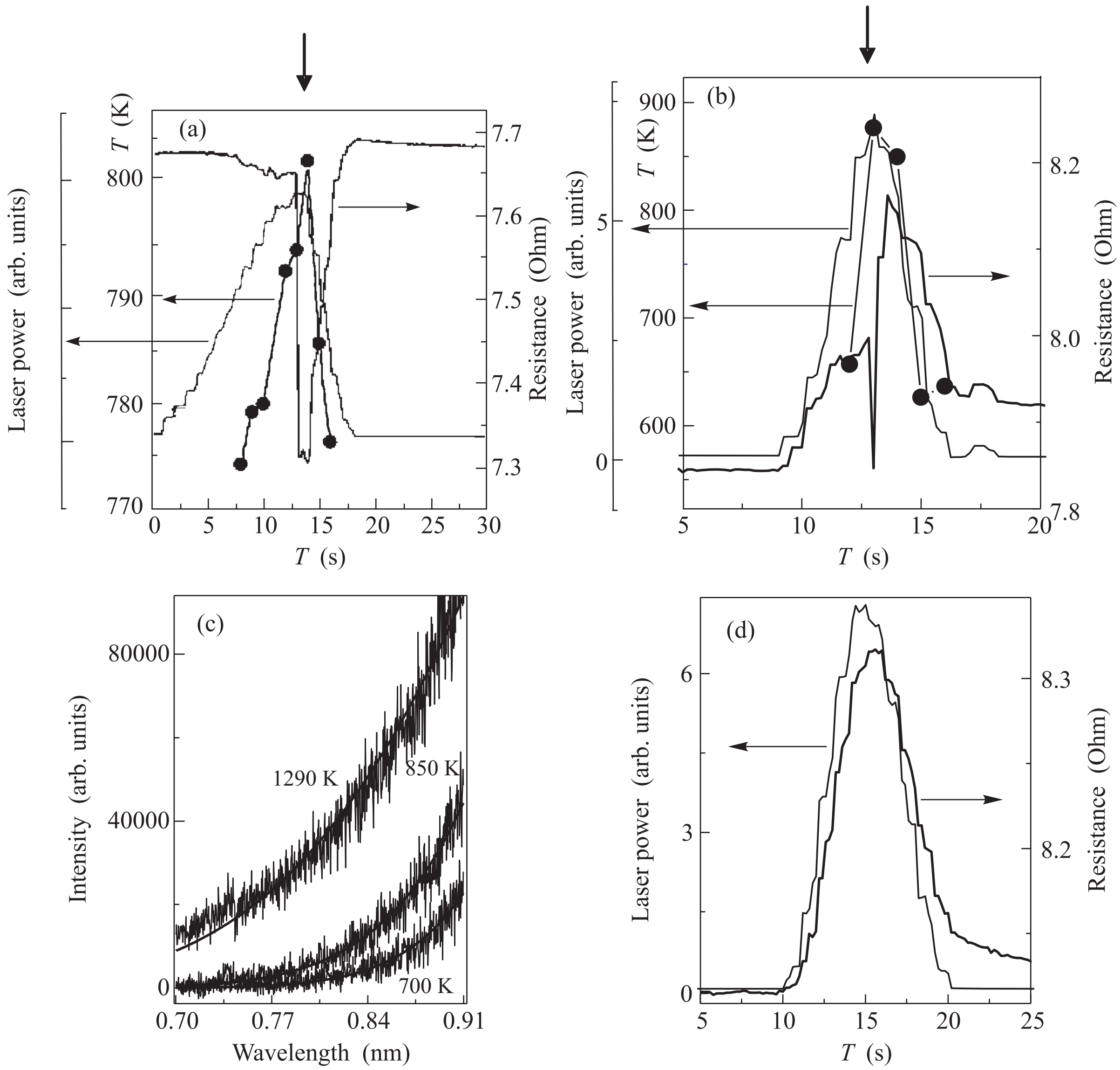

Fig.3. Laser heating of hydrogen at 146 GPa in the diamond anvil cell shown in Fig.2. In typical runs (a), (b), the laser power was increased up to ~ 10 W until the visual detection of melting, then decreased. During each run, temperature (circles), resistance of the Pt foil (thick solid line), and Raman spectra (Fig.4) were measured. The resistance of the Pt foil shows a marked drop of its value coincident with the hydrogen melting (this moment is indicated by vertical arrows). The increase in resistance after the melting (b) or during heating (d) is due to heating of the diamonds as a whole. Temperature was determined from spectra of thermal radiation recorded (c) every 0.5 second

where diamonds are in contact with hot hydrogen [16]. In our study we developed a laser heating technique which allowed for preserving diamond anvils from the deteriorating influence of the hot hydrogen. In this case the temperature of anvils remains almost unchanged (see Figs.2, 3 and the "Discussion Section") while hydrogen can be heated to temperature up to ~ 2000 K in the layer contacting a heater which is in turn insulated with hBN from the anvils. Schematic diagram of the arrangement of a diamond anvil cell for the melting of hydrogen is shown in Fig.2a. The area illuminated with the laser is indicated with the circle in the center while the circle on the right indicates position of the laser in the control experiment described in the text. The photograph (B) shows the diamond anvil cell under light transmitted through the cBN-epoxy gasket, which is transparent at high pressures. The hole (diameter $\approx 20\,\mu$m) in the center of the diamond anvil culets contains hydrogen. The edge of the hole (which is rough in appearance) is a mixture of pieces of cBN gasket and hydrogen. A platinum electrode (1-μm-thick and $\approx$ 5-μm-width foil) passes through the hydrogen sample. The electrode is thermally insulated from the back anvil with a $\sim$ 1-μm-thick transparent piece of hBN. Spacing between the diamonds (thickness of the cBN gasket is estimated as 5–7 μm). The electrode was heated with 5–15 W power 1.054 μm radiation of a YLF-laser focused on a 15–30 μm spot, and thermal radiation spectra were measured every 0.5 seconds from a $3\times3\,\mu m^2$ spot selected by a field diaphragm at the surface of the heated Pt foil. The resistance of the electrode was measured using the quasi-four-probe scheme (each end of the electrode touches two other Pt electrodes extending outside the cell). The Raman spectrum of hydrogen is represented at 300 K and 146 GPa with a vibron line at 4067 cm^{-1}. The signal around 1500 cm^{-1} is Raman scattering from the stressed diamond anvil tip.

Typically in our experiments the laser exposure time was about 30 seconds. This time was sufficient for reliable data acquisition. In a typical laser heating run, we simultaneously measured temperature, resistance of the Pt foil (Fig.3), and Raman spectra (Fig.4).

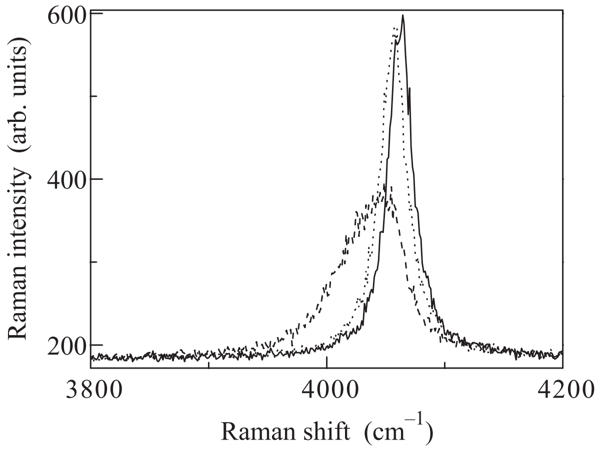

Fig.4. Representative Raman spectra (accumulation time is 0.5 sec) of the hydrogen sample which was laser heated at 146 GPa. In this case the signal was picked up from hydrogen located on the way of the excitation laser beam and heated to different temperatures from $\approx$ 800 K at the surface of the Pt foil down to nearly ambient temperature at the surface of the diamond anvil. The solid line represents the starting spectrum, the dashed line – the spectrum at the maximum of heating which corresponds to the melting of hydrogen the dotted line – the final spectrum collected after the heating run. Numerous intermediate spectra are not shown

Another experimental difficulty is caused by the necessity to measure relatively low values of the melting temperature (e.g., as low as $\approx$ 700 K) at megabar pressures (Fig.1). This is significantly lower than the typical limit (of about 1100 K) of temperature measurement by recording the thermal radiation spectrum and fitting it to the Planck radiation function [22]. This limit is determined mostly by the small amount of emission collected from the micrometer-size sample inside DAC. In order to improve the emission signal we used a specially designed optical-high-throughput setup comprised of a spectrometer equipped with a liquid-nitrogen-cooled charge-coupled device (CCD) detector having an enhanced sensitivity in the near-infrared wavelength region. Spectra were measured in the wavelength range of 0.68–0.92 nm (Fig.3c). This enabled reliable measurements of temperatures using a calibrated tungsten lamp down to 730 K from a spot of $3\times3\,\mu$m and accumulation time of 0.5 sec. The reliability of the low-temperature measurements in the diamond cell was confirmed in experiments with nitrogen and argon, for which melting curves are known from externally heated DAC experiments. We used the experimental assembly similar to that of hydrogen shown in Fig.2. In argon we found $T_{\rm melt} \approx 700-750$ K and $\approx 810-820$ K, at pressures of 5.7 and 7.2 GPa, respectively, which agrees well with the reported in Ref. [15]; in nitrogen, we found $T_{\rm melt} = 830\pm40$ K at 19 GPa, in accordance with data reported in Ref.[23]. We also apply this experimental setup to measure the melting temperature of aluminum ($T_{\rm melt} = 933.5$ K) at ambient pressure.

We determined pressure by measuring the position of the molecular hydrogen vibron peak in Raman scattering spectra at room temperature. This pressure dependent position was calibrated against the ruby scale [24]. We also found the good agreement between values of pressure obtained from the molecular hydrogen vibron position and pressure values determined from the high-frequency edge of the stressed diamond tip [25] taking into account the correction proposed in Ref. [26]. This fact is important as it shows that diamond can be used as a reference for pressure determination during laser heating experiments with hydrogen. We found that position of the high-frequency edge of the upper diamond anvil under pressure remained unchanged (within $\sim 0.5\,cm^{-1}$) giving at 146 GPa a maximum deviation of about 0.5 GPa. Thus the thermal pressure induced by the bulk heating of the sample was negligible, which should be expected if only a small fraction of hydrogen and Pt foil was heated to $T \sim 1000$ K.

3. Experimental results and discussion. In the following section along with results we will address more attentively crucial issues of this work: the assumption that the temperature of diamond anvils remains almost unchanged during the laser heating, and detection of the process of hydrogen melting.

We estimated temperature of diamond anvils by using two temperature indicators contacted the anvils: Pt foil (we measured its resistance), and the hydrogen sample (we measured the temperature shift of the molecular vibron). Starting with the vibron, its position depends not only on temperature but also on pressure. However, pressure did not change during the heating, as we have shown above, therefore the temperature can be directly deduced using the temperature coefficient of the vibron frequency determined at different pressures up to 150 GPa [16]. Unfortunately, we could not measure in such a way the temperature of the melted hydrogen because the molten layer was too thin to be spatially separated from the rest of solid hydrogen with our Raman setup having 180° geometry. Instead, we measured overlapped Raman signals from regions heated to different temperature values. The asymmetric shape of the molecular hydrogen vibron recorded (Fig.4) provides evidence of a large temperature gradient occurring in the hydrogen sample during the laser heating. Moreover, the observed shape asymmetry clearly indicates that only tiny portion of hydrogen was heated to the highest, melting temperatures. The $\approx 20\,\mathrm{cm}^{-1}$ shift of the Raman peak at the maximum heating indicates that hydrogen was heated in average to only $\approx 60\,\mathrm{K}$ as follows from the temperature shift of the vibron ($d\nu/dT = 0.35\,\mathrm{cm}^{-1}/\mathrm{K}$) determined in Ref. [16] at pressures $\sim 150\,\mathrm{GPa}$. The whole hydrogen sample remained warm at $\Delta T \approx 16\,\mathrm{K}$ just after the laser heating run as follows from the shift of the vibron peak at the last spectrum. The sample slowly (minutes) cooled down to the ambient temperature.

The Pt foil can be also used as a common platinum thermometer for monitoring temperature of the anvil. Since diamond has an extremely high thermal conductivity, only little gradients of temperature can occur on the surface as well as in the bulk of diamond – in other words, temperature should be uniform across the diamond surface contacting the hydrogen sample, the gasket and the Pt foil. The Pt thermometer should work also at high pressures because its thermal coefficient ($\alpha \approx 4 \cdot 10^{-3}$) remains almost unchanged (deviation $\sim 10\%$) at 174 GPa [27]. In fact, a part of the Pt foil has been separated from the anvils and used as a heater, and being heated it significantly contributed to the whole resistance. Therefore we estimated the anvil temperature by irradiating Pt foil outside the heater (right circle at Fig.2) with the same power of laser as we used for heating of hydrogen up to $\sim 1000\,\mathrm{K}$. The measured temperature increase of diamond anvil was not higher than $\Delta T \approx 10\,\mathrm{K}$. After the laser irradiation run, the resistance of Pt decreased rapidly to the low value, but slightly higher, if compared to the initial one, indicating the temperature change of the diamond anvil of $\sim 1\,\mathrm{K}$. The complete thermal relaxation takes several minutes according to resistance of Pt, which decreased gradually to the initial value. Summarizing the above, the heating of diamond anvils was low enough to prevent diamond anvil breakage due to penetration of the "hot" hydrogen.

We now discuss on the detection of the melting process along with main results of the work. Although irregular motion of the molten hydrogen was visually detectable our principal method of the hydrogen melting detection was based on the observation of a rapid change in the interference pattern of the reflected light of the heating YLF or argon laser [22]. The interference is caused by different refractive indexes of solid and melt. This high mobility of hydrogen can be expected because it is soft even in solid state – hydrogen is a highly hydrostatic medium at megabar pressures. These methods of detection (visual and interference observations) were also used in the control experiments on nitrogen and argon described above.

In addition to the above mentioned detection methods, we monitored the resistance of the Pt foil during laser heating runs for each pressure. For the pressure of 37, 106 and 140 GPa we detected usual behavior of Pt resistance as a function of the laser power and temperature (similar to that presented in Fig.3d) in contrast to the highest pressure run of 146 GPa: its resistance strongly dropped at the moment of the observed melting indicated by arrows at Figs.3a, b. This helped us to unambiguously determine the melting temperature measured at the moment of the sharp drop in resistance. At 146 GPa we performed the most extensive set of measurements with about 100 heating runs. At this pressure, $T_{\mathrm{melt}} = 880\,\mathrm{K}$ was repeatedly obtained with accuracy better than $\pm 50\,\mathrm{K}$. At other pressures we did not observe the discontinuity in resistance of the Pt foil at the moment of melting; therefore the melting temperature was determined less precisely (Fig.1). Our melting points are shown in Fig.1 with bars which represent error bars. A source of uncertainty of the temperature measurements is an insufficient accumulation time of the emission spectra and consequent scattering of the fitted temperatures. Also, there is an uncertainty in correlation of the measured temperature and the moment of the observed melting. This error was minimal at the 146 GPa run where the moment of melting was clearly assigned to a drastic change in resistance of platinum (Fig.3a, b).

We now comment an intriguing drop in resistance of the platinum foil associated with melting of hydrogen observed at high pressure in the 146 GPa run (Fig.3). It is apparently related to dramatic changes in the surrounding fluid hydrogen. As soon as hydrogen melts at pressures above ~ 150 GPa molecules rapidly dissociate with temperature according to calculations [7, 9, 11]. Therefore atomic hydrogen (protons) can penetrate the bordering Pt foil causing a change of resistance; however, negligible hydrogen is dissolved in Pt (in contrast to Pd), even at 9 GPa and 520 K [28]. But, if platinum hydride does form at megabar pressures, the resistance would increase with increasing concentration of dissolved protons, which are additional scatterers of electrons. A drop in resistance might also occur, but only within a narrow temperature range in the case that the concentration of protons increases such that stoichiometric PtH is attained. In such a case, the scattering of electrons decreases due to the ordering of protons in the Pt lattice [29].

Alternative explanation of the resistance drop at pressures at ~ 150 GPa may be due conductive surrounding hydrogen that shunts the foil. A metallic-like state might appear due to narrowing of the band gap with increasing temperature [7, 9, 11]. Currently available experimental data are insufficient to enable us to discriminate among the above scenarios. We do note, however, that the observed drop in resistance (Fig.3a, b) can be explained by the shunting of a 1–2-μm-thick layer of the conductive hydrogen at the surface of the heated foil, based on a conductivity of $1-2\times10^4 \Omega^{-1}\,\mathrm{cm}^{-1}$, as calculated in Refs [7, 11, 30]. We found that the drop in resistance at the point of hydrogen melting was less pronounced at 140 GPa, and absent at 106 GPa and lower pressures, as well as observed in the melting experiments described above involving argon and nitrogen. These facts are also consistent with calculations [6, 7, 9] that predict conducting molten hydrogen at pressures above $\approx 130-150$ GPa. Direct measurements of conductivity are required to confirm this explanation.

4. Conclusions. We found experimentally an unusual behavior of the melting temperature with pressure: above approximately 100 GPa the melting temperature decreases with rising pressure (Fig.1). This finding is in agreement with theoretical calculations of the melting curve of hydrogen [1].

We are thankful to R. Boehler, Yu. Freiman, T. Palasyuk, and V. Hillgren for valuable discussions, I. Goncharenko and V. Antonov for consulting with us on points of interest, and the DFG grant ER 539/2-1 for a partial support.

1. S. A. Bonev et al., Nature **431**, 669 (2004).
2. V. V. Kechin, JETP Letters **79**, 46 (2004).
3. N. Ashcroft, J. Phys. Condens. Matter A **12**, 129 (2000).
4. E. G. Brovman, Y. Kagan, and A. Kholas, Sov. Phys. JETP **35**, 783 (1972).
5. E. Babaev, A. Sudbo, and N. W. Ashcroft, Nature **431**, 666 (2004).
6. S. Scandolo, PNAS **100**, 3051 (2003).
7. O. Pfaffenzeller and D. Hohl, J. Phys.: Condens. Matter **9**, 11023 (1997).
8. A. Alavi, M. Parrinello, and D. Frenkel, Science **269**, 1252 (1995).
9. J. Vorberger et al., Phys. Rev. B **75**, 024206 (2007).
10. T. J. Lenosky et al., Phys. Rev. B **55**, R11 907 (1997).
11. B. Jakob et al., Phys. Rev. E **76**, 036406 (2007).
12. C. Attaccalite and S. Sorella, Phys. Rev. Lett. **100**, 114501 (2008).
13. W. v. Gulik and W. K. Keesom, Commun. Phys. Lab. Univ. Leiden B **192**, 11 (1928).
14. V. Diatschenko et al., Phys. Rev. B **32**, 381 (1985).
15. F. Datchi, P. Loubeyre, and R. LeToullec, Phys Rev. B **61**, 6535 (2000).
16. E. Gregoryanz et al., Phys. Rev. Lett. **90**, 175701 (2003).
17. S. Deemyad and I. F. Silvera, Phys. Rev. Lett. **100**, 155701 (2008).
18. F. Simon and G. Glatzel, Z. Anorg. Allg. Chem. **178**, 309 (1929).
19. E. A. Kraut and G. C. Kennedy, Phys. Rev. **151**, 668 (1966).
20. S. T. Weir, A. C. Mitchell, and W. J. Nellis, Phys. Rev. Lett. **76**, 1860 (1996).
21. W. J. Nellis, Rep. Prog. Phys. **69**, 1479 (2006).
22. R. Boehler, M. Ross, and D. B. Boercker, Phys. Rev. Lett. **78**, 4589 (1997).
23. S. C. Schmidt et al., J. Appl. Phys. **69**, 2793 (1991).
24. P. Loubeyre, F. Occelli, and R. LeToullec, Nature **416**, 613 (2002).
25. M. I. Eremets, J. Raman Spectroscopy **34**, 515 (2003).
26. B. J. Baer, M. E. Chang, and W. J. Evans, J. Appl. Phys. **104**, 034504 (2008).
27. M.I. Eremets et al., Science Suppl. Mater. **319**, 1506 (2008).
28. V. E. Antonov et al., Intern. J. Hydrogen Energy **11**, 93 (1986).
29. A. Driessen et al., J. Phys.: Condens. Matter **2**, 9797 (1990).
30. R. Q. Hood and G. Galli, J. Chem. Phys. **120**, 5691 (2004).